



Assembly–disassembly switching of self-sorted nanotubes forming dynamic 2-D porous heterostructure†

Xin Liu, Huichang Li, Yongju Kim and Myongsoo Lee *

Cite this: *Chem. Commun.*, 2018, 54, 3102

Received 9th February 2018,
Accepted 21st February 2018

DOI: 10.1039/c8cc01177j

rsc.li/chemcomm

We report the pH-driven formation of a dynamic 2-D porous heterostructure through assembly–disassembly switching of the stacked macrocycles of nanotubes and their subsequent spreading on the surfaces of a self-sorted sheet assembly in a hierarchical co-assembly. The 2-D ordered porous heterostructure is able to discriminate spherical C₆₀ from flat coronene through shape selective adsorption.

Self-assembled 2-dimensional (2-D) heterostructures on solid surfaces have gained widespread interest because their fundamental significance and potential applications.^{1,2} In particular, 2-D networks with void spaces on their surfaces have been explored in various applications, such as molecular separation, electronic devices, and asymmetric catalysts.^{3–6} Mostly, 2-D network structures are formed through self-assembly processes of molecular subunits on a variety of different solid substrates, including semiconductors, metal insulators, and layered materials.^{7–10} In addition to their noncovalent preparation, another attractive aspect of 2-D structures is the possibility that they can dynamically respond to external stimuli.^{11–13} However, such a deposition approach on solid substrates makes the networks insensitive to environmental changes. To create heterostructures which are dynamically responsive to environmental changes, it is necessary to design hierarchical hetero-assemblies that are sensitive to small changes in the interactions on their interfaces while maintaining their sub-nanostructures without breaking.

Given that aromatic macrocycles are intrinsic pore structures,^{14–17} one ideal candidate for the construction of 2-D porous structures is their lateral-assembly into an extended flat nanostructure. In most cases, however, the macrocycles stack on top of one another through strong stacking interactions to generate hollow tubules.¹⁸ For example, non-covalent macrocycles based on bent-shaped aromatic molecules stack on top of each other to generate tubular structures.¹⁹ In this tubular system, the

incorporation of a pyridine unit into the bent-shaped aromatic segment endows the nanostructures with switchable motion through reversible hydrogen bonding interactions.^{20–22}

We envisioned that the aromatic interactions between these stacked macrocycles would be weakened when the pyridine units in the tubules are protonated with a reduction in pH. Consequently, the loosened macrocycle stacks are able to dissociate into discrete macrocycles due to electrostatic repulsion.²³ When faced with negatively-charged planar surfaces, the subsequent electrostatic spreading of the positively-charged macrocycles might generate dynamic 2-D porous heterostructures (Fig. 1).

Here we report the pH-driven formation of a dynamic 2-D porous heterostructure through assembly–disassembly switching of the stacked macrocycles of nanotubes and their subsequent spreading on the surfaces of a self-sorted sheet assembly in a hierarchical co-assembly. The co-assembly is composed of a mixed solution of **1** which forms a tubular structure and carboxylate rod molecules **2** with a high propensity to form flat 2-D sheet structures.²⁴ When mixed in an aqueous solution under neutral conditions (pH 7.4), **1** and **2** self-sort into tubules and 2-D sheets, respectively. Upon lowering the pH to 5.5, the self-sorted tubules of **1** disassemble into their constituent macrocycles, which spontaneously spread out on the sheet surfaces of **2** with a hexagonal lattice to generate a 2-D porous heterostructure (Fig. 1). Interestingly, the 2-D porous heterostructure is able to readily discriminate spherical C₆₀ from flat coronene through selective adsorption from a mixed solution.

The amphiphilic molecules, **1** and **2**, were synthesized in a stepwise fashion according to the procedure described in the ESI† (Fig. S1–S3). **1** based on a bent-shaped aromatic segment self-assembled into a tubular structure with an external diameter of ~7 nm in aqueous solution (Fig. 2a). The dimension of the diameter indicates that the tubules are based on the stacking of hexameric macrocycles (Fig. 2d), similar to the results reported previously.^{20,21} The formation of tubular structures is also confirmed by AFM (Fig. S4, ESI†), which is consistent with the result obtained from TEM. On the other hand, **2** is based on rod-shaped molecules self-assembled into flat sheets in

State Key Lab of Supramolecular Structure and Materials, College of Chemistry, Jilin University, Changchun 130012, China. E-mail: mslee@jlu.edu.cn

† Electronic supplementary information (ESI) available. See DOI: 10.1039/c8cc01177j

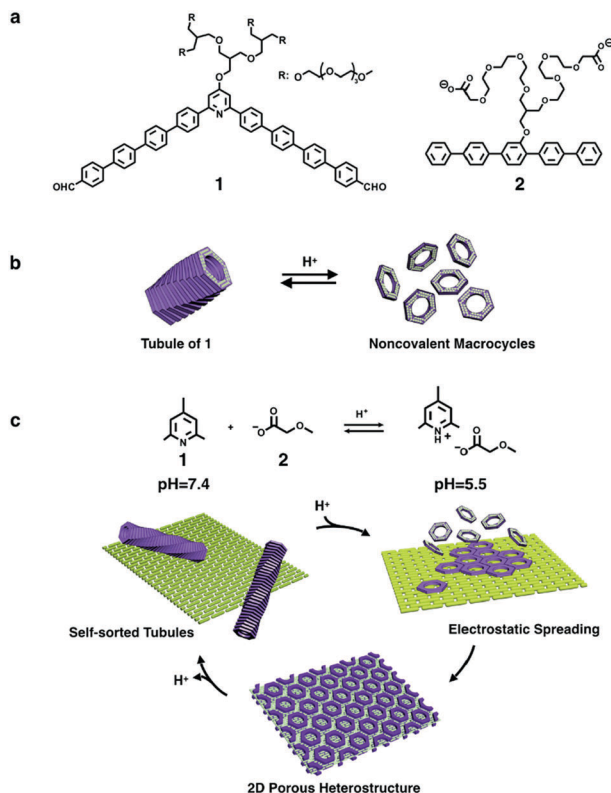


Fig. 1 (a) Molecular structure of **1** and **2**. (b) pH-responsive cutting of tubules **1** into non-covalent macrocycles. (c) Schematic representation of co-assembly of **1** and **2** into self-sorted tubules and sheets, respectively, at pH = 7.4, which are merged to form 2-D network heterostructures at pH = 5.5.

aqueous solution. TEM showed isolated sheet objects with straight edges, ranging in lateral dimensions from submicro- to several micrometers, indicating that the sheets are robust (Fig. 2b). To obtain more information on the sheets, we additionally performed cryo-TEM experiments, which showed flat 2-D structures (Fig. S5, ESI[†]), demonstrating that the sheets are free standing in bulk solution. AFM analysis revealed that the sheets are very flat and uniform with a thickness of 2.8 nm (Fig. 2c and Fig. S6, ESI[†]). This result indicates that the aromatic rods of **2** are packed in a monolayer arrangement with carboxylate anion surfaces in which the rods are aligned parallel to the sheet plane (Fig. 2d).

We anticipated that a mixed solution of **1** and **2** would produce self-sorted tubules and 2-D sheets, respectively, due to steric incompatibility between the bent-shaped and rod-shaped aromatic segments.²⁵ To corroborate this self-sorting behavior, we prepared a solution of a 1:1 mixture of **1** and **2** in CHCl₃, slowly removed the organic solvent and added phosphate buffer under ambient conditions. TEM investigations of the mixed solution under neutral conditions (pH 7.4) revealed the coexistence of tubules and flat sheets (Fig. S7, ESI[†]), indicating that **1** and **2** self-recognize to form two distinct self-sorted structures. The self-sorting behavior was further confirmed by fluorescence measurements of the mixed solution, which revealed a lack of fluorescence quenching of **2** (Fig. S8, ESI[†]).

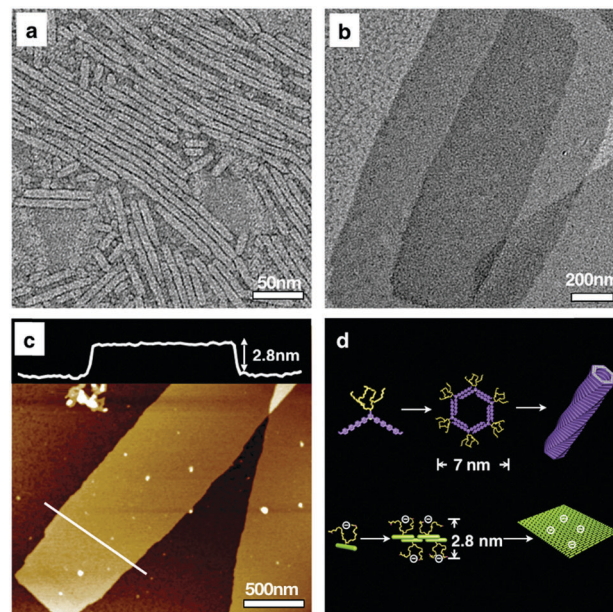


Fig. 2 Self-assembled nanostructures of **1** and **2** in aqueous solution. (a) Negatively-stained TEM image of **1** (30 μM). (b) Negatively-stained TEM image of **2** (60 μM). (c) AFM height image of sheets on a mica surface from evaporated film of **2** (60 μM) in aqueous solution. The cross-sectional profile (top) is shown by the white line. (d) Schematic representation of tubules of **1** and sheets of **2** at pH 7.4.

Considering that the pK_a value of the pyridine unit in molecule **1** is 5.8,²² decreasing the pH value to 5.5 would lead to the pyridine units being partially protonated, and so they would become positively charged in the tubular interior. Consequently, the positive charges might reduce the attractive interactions among the constituent hexameric macrocycle stacks due to electrostatic repulsion. Upon lowering the pH to 5.5, the tubules indeed dissociate into their constituent non-covalent macrocycles. TEM at pH 5.5 revealed toroidal objects with a uniform diameter of ~7 nm (Fig. S9, ESI[†]). This value is similar to the diameter of the tubule, indicating that the macrocyclic objects form as a result of the repulsive dissociation of the tubules at a lower pH value. On the other hand, the sheet surfaces of **2** would be coated with negative charges at this pH value (carboxylic acid pK_a of 4.7), which would allow the 2-D structure to form a hierarchical co-assembly with positively-charged objects. To monitor the electrostatic couplings between the positively-charged macrocycles of **1** and the negatively-charged 2-D surfaces of **2**, we carried out fluorescence measurements upon addition of the tubular solution of **1** into the sheet solution of **2** at pH 5.5 (Fig. S10, ESI[†]). As the amount of **1** increases, the emission of **2** excited at the absorption maximum of **2** gradually decreases at 388 nm, with the simultaneous appearance of the fluorescence emission associated with **1** centered at 442 nm, indicating efficient energy transfer between the two molecules.²⁶ This result demonstrates the formation of a complex of **1** and **2** through electrostatic interactions at pH 5.5. The optimum condition for the formation of the complex was achieved at a molar ratio ([**1**]/[**2**]) of 0.5. These results imply that the tubule of

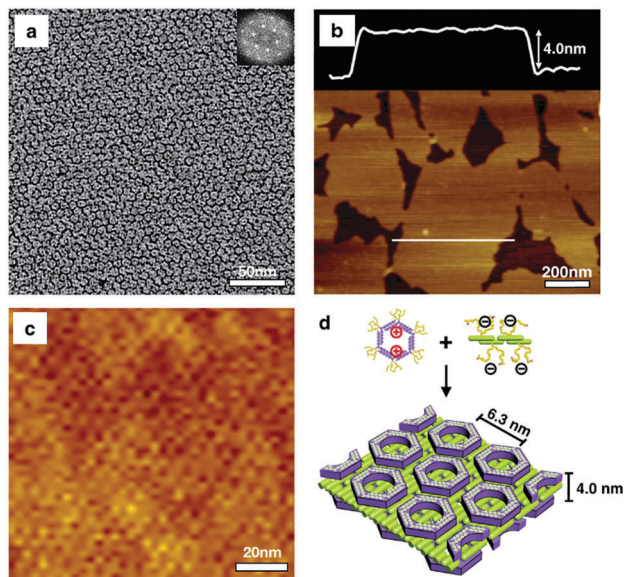


Fig. 3 (a) Negatively-stained TEM image of a mixed solution ($[1]/[2] = 0.5$) at pH 5.5. The inset shows the 2-D Fourier transformation of a hexagonal structure. (b) AFM height image of a mixed solution ($[1]/[2] = 0.5$) at pH 5.5. The cross-sectional profile (top) is shown by the white line. (c) High resolution AFM image of a mixed solution ($[1]/[2] = 0.5$) at pH 5.5. (d) Schematic representation of the 2-D network heterostructure at pH 5.5.

1 would dissociate into its constituent macrocycles with a positively-charged interior to spread on the negatively-charged sheet surfaces of **2**.

To corroborate the structural transformation upon lowering the pH, we performed TEM investigations with a mixed solution ($[1]/[2] = 0.5$) at pH 5.5. Upon lowering the pH to 5.5, TEM indeed showed the formation of a 2-D hexagonally-ordered porous structure at the expense of the tubules, with a center to center distance of 6.5 nm (Fig. 3a and Fig. S11, ESI[†]), which is slightly less than the tubular size in diameter. This result demonstrates that the tubules dissociate into their constituent macrocycles, which are deposited with a closely-packed 2-D hexagonal array on the negatively-charged surfaces. The AFM image at pH 5.5 revealed flat sheet structures with the thickness increasing from 2.8 nm to 4.0 nm (Fig. 3b). This increase in thickness is consistent with twice the expected molecular thickness of **1**, indicating that the top and bottom surfaces of the sheet are coated with lateral arrangements of the constituent macrocycles. The high resolution AFM image revealed an in-plane hexagonal order of the pores, with a center to center distance of 6.3 nm, which is consistent with the results obtained from TEM (Fig. 3c and Fig. S12, ESI[†]). This result suggests that the weakened macrocycle stacks at the lower pH dissociate into single macrocycles which are electrostatically spread parallel to the layer surfaces with a closely-packed 2-D hexagonal symmetry (Fig. 3d).

On the basis of these results, the most probable mechanism responsible for the generation of the 2-D porous heterostructure can be illustrated as shown in Fig. 1c. The mixed solution of **1** and **2** under neutral conditions co-exists in two distinct self-sorted structures, that is, tubules and flat sheets. Upon lowering the pH, however, the macrocycle stacks of the tubules

would be loosened because of the protonation of the tubule interior. This is supported by the remarkable fluorescence enhancement of **1** upon a change in pH from 7.4 to 5.5 (Fig. S13, ESI[†]). Consequently, the loosely-packed tubules dissociate into the constituent macrocycles which are spread on the negatively-charged 2-D surfaces, generating a 2-D hexagonally-ordered porous heterostructure.

The 2-D ordered porous structures with hollow aromatic cavities can be expected to encapsulate aromatic hydrocarbon molecules (Fig. 4a and Fig. S14, ESI[†]).⁴ We select spherical C_{60} and flat coronene as guest candidates because of their similar diameters (1.1 nm) but different shapes.²⁷ Upon addition of C_{60} into the porous structure solution, the fluorescence emission associated with the 2-D structure gradually decreased up to 2.0 eq. of the guest and then levelled off (Fig. 4b and Fig. S15, ESI[†]), indicating that the porous heterostructure can include a maximum amount of approximately two C_{60} molecules per cavity. In great contrast, when coronene was added, fluorescence emission revealed no noticeable changes (Fig. S16, ESI[†]), demonstrating that the porous heterostructure is unable to host the coronene guest. The shape selectivity of the 2-D porous structure could result from a steric mismatch between the shallow cavity and the aromatic guest. In the case of the coronene guest, the flat aromatic core would be oriented edge-on to the charged surfaces.²⁸ Consequently, the guest-cavity interactions would not be strong enough for the coronene guest to reside inside the cavities due to the larger steric mismatch between the curved cavity walls and the planar guest core. Considering the similar size in diameter of coronene and C_{60} , this result indicates that the 2-D porous structures are able to adsorb aromatic hydrocarbon guests with shape selectivity. It is worth noting that the 2-D porous structure readily captures the C_{60} guest within 5 min, in great contrast to the tubules which are unable to encapsulate C_{60} within

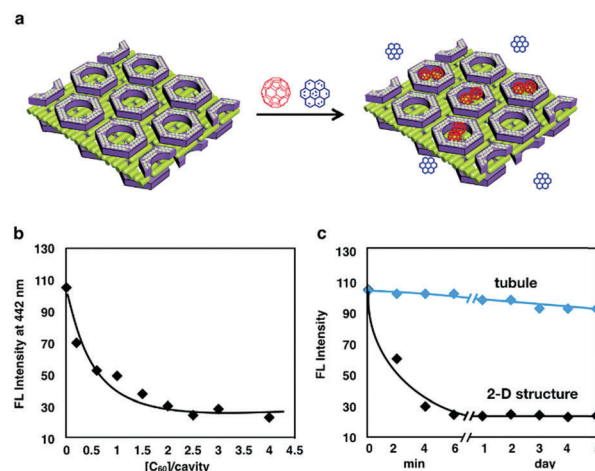


Fig. 4 (a) Schematic representation of guest adsorption with shape selectivity by the 2-D porous heterostructure. (b) Emission spectra intensities of different equivalents of C_{60} per cavity based on $30 \mu\text{M}$ **1** at pH 5.5. Excitation wavelength: 330 nm. (c) Time dependent emission intensity for encapsulation of 2.0 eq. of C_{60} . The blue line represents the tubule structure encapsulating C_{60} and the black line represents the heterostructure encapsulating C_{60} .

this time period (Fig. 4c). This is because all the pores in the 2-D structure are exposed to the external environment, unlike the tubules with only the two openings at either end. This result indicates that the 2-D assembly of macrocycle containers is essential for the efficient encapsulation of hydrophobic guests in aqueous solution.

Our work demonstrates that 2-D ordered porous heterostructures can be formed by the reversible dissociation of a self-assembled tubule into its constituent macrocycles and simultaneous spreading on a self-sorted sheet surfaces in a co-assembly solution. Under neutral conditions (pH 7.4), the co-assembly of a bent-shaped aromatic segment, **1** and a rod-shaped segment of **2** generates the coexistence of self-sorted tubules and 2-D sheets, respectively. Upon lowering the pH to 5.5, however, the self-sorted tubules dissociate into their constituent macrocycles, which are spontaneously spread on the negatively-charged sheet surfaces of **2** to form a 2-D hexagonally-ordered porous heterostructure. The ordered porous heterostructures are able to discriminate spherical C₆₀ from flat coronene through shape selective adsorption, which functions as a filter to capture only a spherical-shaped molecule.

This work was supported by 1000 Program, JLUSTIRT, NSFC (Grant 51473062 and Grant 21450110416).

Conflicts of interest

There are no conflicts to declare.

Notes and references

- W. Chen, D. C. Qi, H. Huang, X. Gao and A. T. S. Wee, *Adv. Funct. Mater.*, 2011, **21**, 410.
- A. Hinderhofer and F. Schreiber, *ChemPhysChem*, 2012, **13**, 628.
- J. W. Colson, A. R. Woll, A. Mukherjee, M. P. Levendorf, E. L. Spitler, V. B. Shields, M. G. Spencer, J. Park and W. R. Dichtel, *Science*, 2011, **332**, 228.
- M. O. Blunt, J. C. Russell, M. C. Gimenez-Lopez, N. Taleb, X. Lin, M. Schröder, N. R. Champness and P. H. Beton, *Nat. Chem.*, 2011, **3**, 74.
- T. Chen, W. Yang, D. Wang and L. Wan, *Nat. Commun.*, 2013, **4**, 1389.
- T. Kudernac, S.-B. Lei, J. A. A. W. Elemans and S. De Feyter, *Chem. Soc. Rev.*, 2009, **38**, 402; G. Schull, L. Douillard, C. Fiorini-Debuisschert and F. Charra, *Nano Lett.*, 2006, **6**, 1360.
- S. Jiang, Q. Song, A. Massey, S. Y. Chong, L. Chen, S. Sun, T. Hasell, R. Raval, E. Sivaniah, A. K. Cheetham and A. I. Cooper, *Angew. Chem., Int. Ed.*, 2017, **56**, 9391.
- V. V. Korolkov, M. Baldoni, K. Watanabe, T. Taniguchi, E. Besley and P. H. Beton, *Nat. Chem.*, 2017, **9**, 1191.
- O. Stetsovych, M. Švec, J. Vacek, J. V. Chocholoušová, A. Jančařík, J. Rybáček, K. Kosmider, I. G. Stará, P. Jelínek and I. Starý, *Nat. Chem.*, 2016, **9**, 213.
- K. Tahara, H. Yamaga, E. Ghijssens, K. Inukai, J. Adisojoso, M. O. Blunt, S. De Feyter and Y. Tobe, *Nat. Chem.*, 2011, **3**, 714.
- H. Kim, T. Kim and M. Lee, *Acc. Chem. Res.*, 2011, **44**, 72.
- Y. Wang, Y. Kim and M. Lee, *Angew. Chem., Int. Ed.*, 2016, **55**, 13122.
- B. Shen, Y. He, Y. Kim, Y. Wang and M. Lee, *Angew. Chem., Int. Ed.*, 2016, **55**, 2382.
- M. Iyoda and H. Shimizu, *Chem. Soc. Rev.*, 2015, **44**, 6411.
- Z. He, X. Xu, X. Zheng, T. Ming and Q. Miao, *Chem. Sci.*, 2013, **4**, 4525.
- W. Zhang and J. S. Moore, *Angew. Chem., Int. Ed.*, 2006, **45**, 4416.
- S. Lee, C.-H. Chen and A. H. Flood, *Nat. Chem.*, 2013, **5**, 704.
- X. Zhou, G. Liu, K. Yamato, Y. Shen, R. Cheng, X. Wei, W. Bai, Y. Gao, H. Li, Y. Liu, F. Liu, D. M. Czajkowsky, J. Wang, M. J. Dabney, Z. Cai, J. Hu, F. V. Bright, L. He, X. Zeng, Z. Shao. and B. Gong, *Nat. Commun.*, 2012, **3**, 949; M. Iyoda and H. Shimizu, *Chem. Soc. Rev.*, 2015, **44**, 6411.
- H. Kim, S.-K. Kang, Y.-K. Lee, C. Seok, J.-K. Lee, W.-C. Zin and M. Lee, *Angew. Chem., Int. Ed.*, 2010, **49**, 8471.
- Z. Huang, S.-K. Kang, M. Banno, T. Yamaguchi, D. Lee, C. Seok, E. Yashima and M. Lee, *Science*, 2012, **337**, 1521.
- Y. Wang, Z. Huang, Y. Kim, Y. He and M. Lee, *J. Am. Chem. Soc.*, 2014, **136**, 16152.
- Y. Kim, H. Li, Y. He, X. Chen, X. Ma and M. Lee, *Nat. Nanotechnol.*, 2017, **12**, 551.
- T. Fukino, H. Joo, Y. Hisada, M. Obana, H. Yamagishi, T. Hikima, M. Takata, N. Fujita and T. Aida, *Science*, 2014, **344**, 499.
- E. Lee, J.-K. Kim and M. Lee, *Angew. Chem., Int. Ed.*, 2009, **48**, 3657.
- M. M. S. Sempere, G. Fernández and F. Würthner, *Chem. Rev.*, 2011, **111**, 5784; K. Aratsu, D. D. Prabhu, H. Iwawaki, X. Lin, M. Yamauchi, T. Karatsu and S. Yagai, *Chem. Commun.*, 2016, **52**, 8211.
- D.-W. Lee, T. Kim, I.-S. Park, Z. Huang and M. Lee, *J. Am. Chem. Soc.*, 2012, **134**, 14722.
- R. Qiao, A. P. Roberts, A. S. Mount, S. J. Klaine and P. Ke, *Nano Lett.*, 2007, **7**, 614.
- T. D. Choudhury, N. V. S. Rao, R. Tenent, J. Blackburn, B. Gregg and I. I. Smalyukh, *J. Phys. Chem. B*, 2011, **115**, 609.